01.1;04.4

Magnetic field inside and in the proximity of the toroidal plasma current filament strapped in the equilibrium by an external axial field

© I.V. Sokolov, D.B. Borovikov

University of Michigan, Ann Arbor, USA
E-mail: igorsok@umich.edu

Received February 22, 2023
Revised April 4, 2023
Accepted April 4, 2023

We provide a description of magnetic field inside and outside of a circular plasma ring carrying an electric current. The equilibrium is maintained by an external axial magnetic field. The provided solution is close to that by Titov and Demoilin (1999), but our solution is more general and accurate.

Keywords: flux rope in equilibrium, coronal mass ejection, toroidal coordinates.

DOI: 10.61011/TPL.2023.06.56369.19535

Here we propose a description of an equilibrium plasma current filament applicable in simulating the coronal mass ejection (CME) on the Sun. It is believed that the source of CME in the solar corona may be a segment of a dense toroidal plasma current filament kept in equilibrium by the magnetic field of the Sun's active region (AR). Superimposing such a configuration [1] onto the AR model enables numerical simulation of the initial equilibrium, loss of equilibrium due to instability, and conversion of the filament current energy to the CME kinetic energy [2]. Contrary to the case of applications to the magnetic confinement of plasma, for which complicated analytical solutions in external specially created fields are of interest [3], the proposed simple solution is used as an initial condition for equations of relaxation magnetohydrodynamics (RMHD) whose solution drives the equilibrium to real external fields of AR.

Let us describe axisymmetric magnetic field $\mathbf{B}(\mathbf{R}) = \mathrm{rot}(A_\varphi \mathbf{e}_\varphi)$ ($\mathbf{A} = A_\varphi \mathbf{e}_\varphi$ is the vector potential, $\mathbf{e}_\varphi$ is the coordinate φ unit vector) created by toroidal current $\mathbf{j} = j_\varphi \mathbf{e}_\varphi$ in toroidal coordinates (u, v, φ) that may be expressed in cylindrical coordinates (z, r, φ) in the following way:

$$\sin v = \frac{2R_\infty z}{R_+ R_-}, \quad \cos v = \frac{R^2 - R_\infty^2}{R_- R_+}, \quad \kappa'(u) = \frac{R_-}{R_+},$$

$$H_u = H_v = \frac{R_\infty}{\cosh u - \cos v},$$

where R_∞ is the magnetic axis radius in the $z = 0$ plane where $u \to \infty$; $H_{u,v}$ are the Lamet coefficients; $R = \sqrt{\mathbf{R}^2} = \sqrt{r^2 + z^2}$, $\mathbf{R}$ is the radius-vector from the configuration center to the specified point, and $R_\pm = \sqrt{R^2 + R_\infty^2 \pm 2R_\infty r}$ is the maximal $(+)$ and minimal $(-)$ distance from the point to the magnetic axis. Unit vectors of the toroidal coordinates are defined as follows:

$$\mathbf{e}_v = \frac{(R^2 - R_\infty^2)\mathbf{e}_z - 2\mathbf{R}(\mathbf{R}\cdot\mathbf{e}_z)}{\kappa' R_+^2}, \quad \mathbf{e}_u = \left[\mathbf{e}_v \times \mathbf{e}_\varphi\right]. \quad (1)$$

After the $\psi = (R_\infty r)^{1/2} A_\varphi$ substitution, the Ampere equation $\mathrm{rot}\,\mathrm{rot}\mathbf{A} = \mu_0 \mathbf{J}$ takes the following form:

$$\mu_0 \{H_u H_v J_\varphi\} = \frac{1}{\sqrt{R_\infty r}} \left(-\frac{d^2\psi}{\partial u^2} - \frac{\partial^2 \psi}{\partial v^2} + \frac{3\psi}{4\sinh^2 u} \right), \quad (2)$$

$\{H_u H_v J_\varphi\}$ is the current density normalized to $dudv$. Fourier decomposition (i is the imaginary unit)

$$\psi = \sum_{n=-\infty}^{\infty} \exp(\mathrm{i}nv)\psi_n(u), \;\; J_\varphi = \sqrt{\frac{R_\infty}{r^5}} \sum_{n=-\infty}^{\infty} \exp(\mathrm{i}nv) j_n(u)$$

separates the variables in (2): each field harmonic ψ_n is determined by current harmonic j_n,

$$\frac{d^2\psi_n(u)}{du^2} - \left(n^2 + \frac{3}{4(\sinh u)^2} \right)\psi_n(u) = -\mu_0 R_\infty \frac{j_n(u)}{(\sinh u)^2}. \quad (3)$$

The major and minor radii R_0, a on the plasma filament boundary are related with $R_\infty = \sqrt{R_0^2 - a^2}$, while coordinate $u = u_0$ has a constant value, $\kappa'(u_0) = a/(R_0 + R_\infty)$. Outside the filament, where $\kappa'(u) > \kappa'(u_0)$, the equation (3) right-hand part becomes zero and has a solution in the form of toroidal function $\tilde{P}^{-1}_{n-1/2}(u) = \sqrt{2\sinh u} P^{-1}_{n-1/2}(\cosh u)$, where $P^{-1}_{n-1/2}(\cosh u)$ is the associated Legendre function. Inside the filament, the equation (3) solution gets expressed via functions $\tilde{Q}^{-1}_{n-1/2}(u) = \sqrt{2\sinh u} Q^{-1}_{n-1/2}(\cosh u)$. The toroidal functions are to be calculated via hypergeometric series in terms of powers of κ'. The current integral

$$I = \int_{u_0}^{\infty} \int_0^{2\pi} \{H_u H_v J_\varphi\} dv du = \sum_{n=-\infty}^{\infty} \int_{u_0}^{\infty} \frac{j_n(u)\tilde{Q}^{-1}_{n-1/2}(u)}{(\sinh u)^2} du \quad (4)$$

follows from decomposition [5] of function $[2(\cosh u - \cos v)]^{-1/2}$ and equation (8.734) given in [6].

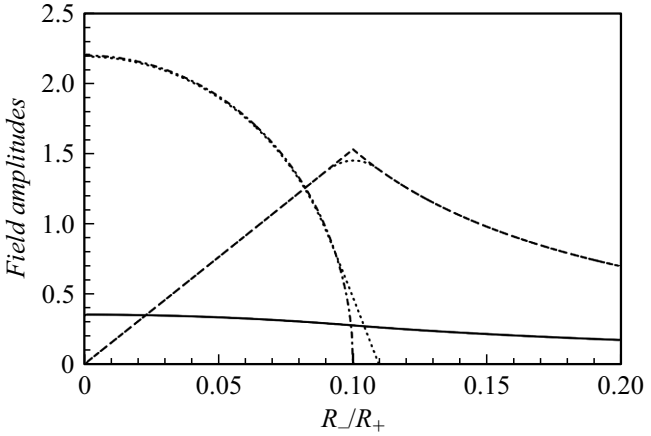

Figure 1. Dimensionless amplitudes of axial field $B^{(z)}(u)$ (solid line), poloidal field $B^{(p)}(u)$ (dashed line) and toroidal field $\frac{b(u)}{B_c}$ (dash-and-dot line) for the toroidal filament with ratio $\frac{a}{R_0} = 0.2$. The function argument $\kappa'(u) = R_-/R_+$ varies inside the filament from zero on the toroidal magnetic axis to $\kappa'(u) = \kappa'(u_0) \approx \frac{a}{2R_0} = 0.1$ on the filament surface; values $\kappa' > 0.1$ correspond to the space outside the filament. The dashed lines represent the option curves for the current distribution which decreases to zero on the boundary in a narrow region near the filament boundary, in distinct with the uniform current distribution (all the other curves) which changes stepwise from a finite value inside the filament to zero outside it.

Let us consider the case when the field has only one harmonic $n = 0$. Hereinafter, index 0 is missed. Poloidal magnetic field outside the filament

$$\mathbf{B} = \frac{4R_\infty}{\kappa^3 R_+^3}\left(\psi \mathbf{e}_z - \frac{\kappa^2}{\kappa'}\frac{d\psi}{du}\mathbf{e}_v\right),$$

$$\frac{\psi(u < u_0)}{\mu_0 R_\infty I} = \frac{\tilde{P}^{-1}_{-1/2}(u)}{8}, \quad \kappa = \sqrt{1-\kappa'^2} \tag{5}$$

coincides with the known field of the infinitely thin circular current (see task 2 to ch. 30 in [7]). For the finite-thickness filament, this conventional solution gets realized if $j \equiv j_0(u)$ (so that $J_\varphi \propto \frac{j_0(u)}{r^{5/2}}$). According to (5) and (6), the field in the center ($\mathbf{R} = 0$) where $\kappa \to 0$, $\tilde{P}^{-1}_{-1/2}(u) \to \frac{\kappa^3}{4}$, $\frac{d\tilde{P}^{-1}_{-1/2}(u)}{du} \to \frac{3\kappa}{4}$, $\kappa' \to 1$, equals $\mathbf{B}_c = \mu_0 I \mathbf{e}_z/(2R_\infty)$. In the proximity of the filament and inside it we have

$$\mathbf{B} = \frac{R_\infty^{3/2}}{r^{3/2}}\left[\frac{2\mathbf{R}(\mathbf{B}_c\cdot\mathbf{R}) + \mathbf{B}_c(R_\infty^2 - R^2)}{R_+^2\kappa'}B^{(p)}(u) + \mathbf{B}_c B^{(z)}(u)\right], \tag{6}$$

where amplitudes of axial field $B^{(z)}(u)$ and poloidal field $B^{(p)}(u)$ normalized to B_c are in essence

$$B^{(z)} \equiv \frac{\psi}{\mu_0 R_\infty I}, \qquad B^{(p)} = \frac{\kappa^2}{\kappa'}\frac{dB^{(z)}}{du}. \tag{7}$$

If the current density inside the filament is uniform, $j(u > u_0) = -3I/[4d\tilde{Q}^{-1}_{-1/2}(u_0)/du_0]$, the equation (3) solution is represented by a sum of the partial (constant) and general solutions of the homogeneous equation $\propto Q^{-1}_{-1/2}(u)$ which ensures the field continuity at $u = u_0$:

$$B^{(z)}(u < u_0) \equiv \frac{\psi}{\mu_0 R_\infty I},$$

$$B^{(p)}(u > u_0) = \frac{\kappa^2}{8\kappa'}\frac{d\tilde{P}^{-1}_{-1/2}(u_0)/du_0}{d\tilde{Q}^{-1}_{-1/2}(u_0)/du_0}\frac{d\tilde{Q}^{-1}_{-1/2}(u)}{du},$$

$$\frac{\psi(u > u_0)}{\mu_0 R_\infty I} = \frac{d\tilde{P}^{-1}_{-1/2}(u_0)/du_0}{8d\tilde{Q}^{-1}_{-1/2}(u_0)/du_0}\tilde{Q}^{-1}_{-1/2}(u) - \frac{1}{d\tilde{Q}^{-1}_{-1/2}(u_0)/du_0}. \tag{8}$$

Fig. 1 presents amplitudes (8) for a filament with $a/R_0 \approx 0.2$. Other partial solutions of equation (3) for the zero harmonic ($n = 0$) of the field $\psi_0 \sim P_m(\coth u)$ arise if the current distribution may be fitted by Legendre polynomial $j_0(u) \sim P_m(\coth u)$ with argument $\coth u = \frac{R_+^2 + R_-^2}{R_+^2 - R_-^2}$; the solution for the current representable as a linear combination of Legendre polynomials is more cumbersome. Remember that the uniform current distribution giving rise to equation (8) matches the zero-order Legendre polynomial: $P_0(\coth u) = 1$.

The equilibrium is controlled by toroidal field $\pm B_\varphi \mathbf{e}_\varphi$ and plasma pressure, which we assume to be $B_\varphi^2 = b^2(u)R_\infty^3/r^3$, $P = p(u)R^3/r^3$. The force normalized to unit volume implies the poloidal field effect on toroidal current

$$J_\varphi \mathbf{e}_\varphi \times \mathbf{B} = \frac{j(u)\sinh u}{r^4}\frac{d\psi}{du}\mathbf{e}_u + \frac{J_\varphi A_\varphi}{2r}\mathbf{e}_r, \tag{9}$$

as well as the toroidal field impact on poloidal current and pressure gradient is

$$\frac{\mathrm{rot}(B_\varphi e_\varphi)}{\mu_0} \times B_\varphi \mathbf{e}_\varphi - \nabla P = -\frac{R_\infty^3 \sinh u}{r^4}\frac{dp_{tot}(u)}{du}\mathbf{e}_u + \frac{3P + B_\varphi^2/(2\mu_0)}{r}\mathbf{e}_r, \tag{10}$$

where $p_{tot}(u) = p(u) + \frac{b^2(u)}{2\mu_0} = (1+\beta)\frac{b^2}{2\mu_0}$ is the the total pressure. The total force directed along $\mathbf{e}_u$ disappears when $R_\infty^3 dp_{tot}/d\psi = j(u)$. For the uniform current $j(u)$, integration provides

$$p_{tot}(u) = \frac{3B_c^2}{8\mu_0}\frac{d\tilde{P}^{-1}_{-1/2}(u_0)/du_0}{[d\tilde{Q}^{-1}_{-1/2}(u_0)/du_0]^2}\left[\tilde{Q}^{-1}_{-1/2}(u_0) - \tilde{Q}^{-1}_{-1/2}(u)\right]. \tag{11}$$

The pressure difference between the filament depth and surface is counterbalanced by the toroidal current pinch-effect. If $\beta = 2\mu_0 p(u)/b^2(u)$, equilibrium (11) is completely governed by distribution of the toroidal field whose amplitude $b(u)/B_c$ is shown in Fig. 1. Peculiarities of amplitudes

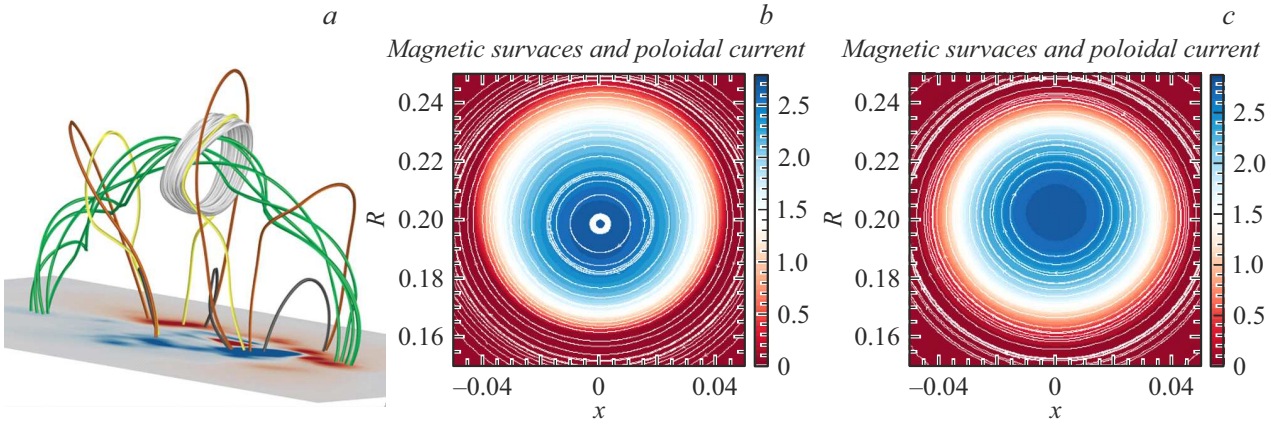

Figure 2. The result of applying the obtained solution to describing CME 2013-04-11. The plasma filament major and minor radii $R_0 = 0.2$, $a = 0.04$ are normalized to the solar radius, Karrington longitude and latitude of the configuration center are $2135 : 79.8^\circ$ and 12.8°, respectively. *a* — force lines of the total AR magnetic field and superimposed current-carrying plasma configuration. The green bundle of twisted magnetic lines illustrates the plasma filament internal field. Lines of other colors represent force lines of external fields of different topologies. The red and blue colors on the (horizontal) solar surface represent AR-forming sunspots of positive and negative polarity. *b* — magnetic fields in the current filament meridional cross-section: white curves are the lines of poloidal field (B_z, B_r) (the same are cross-sections of magnetic surfaces), the color indicates the level of the rB_φ value proportional to the poloidal current. *c* — the same as above but after the RMHD relaxation during 6000 s. The equi-current lines ideally coincide with the magnetic surfaces thus demonstrating the equilibrium character of the obtained configuration. The colored figure is given in the electronic version of the paper.

on the filament boundary (vertical asymptote in the toroidal field amplitude, a jump of derivative in the poloidal field amplitude) disappear if in a minor neighborhood of the boundary there is introduced current distribution $j_0 \sim [\coth(u_0 - \varepsilon) - \coth u]$, $u_0 - \varepsilon < u < u_0 + \varepsilon$, $\varepsilon \ll 1$ becoming zero at the filament boundary.

Resulting force $\mathbf{f}_r \parallel \mathbf{e}_r$ obtained by summing (9) and (10) tends to extend the filament in the $\mathbf{e}_r$ direction. The filament may be prevented against expansion by external field $\mathbf{B}^{(str)} = B^{(str)}\mathbf{e}_z$ which can be estimated (see [3,8]) by integrating, over the filament volume, the sum of the extending and confining forces $\mathbf{f}_r + J_\varphi \mathbf{e}_\varphi \times \mathbf{B}^{(str)}$ scalarly multiplied by $\mathbf{R}$ (such an integral estimation is referred to as Shafranov's virial theorem [9]), the volume element being $dV = rd\varphi dS$:

$$\int (\mathbf{f}_r \cdot \mathbf{R} + J_\varphi r B^{(str)}) dV = \int \left(\frac{j_\varphi A_\varphi}{2} + \frac{B_\varphi^2}{2\mu_0} + 3P \right) dV$$

$$+ 2\pi B^{(str)} I R_\infty^2 \approx \frac{LI^2}{2} + 2\pi B^{(str)} I R_\infty^2. \tag{12}$$

At constant β, the first integral is expressed through the magnetic field energy, which makes it possible to define it as $\frac{1}{2}LI^2$ (where L is the inductance) and estimate the confining field

$$B^{(str)} \approx -\frac{LI}{4\pi R_\infty^2},$$

$$L = \frac{2}{I^2} \int \left[\frac{j_\varphi A_\varphi}{2} + \frac{B_\varphi^2}{2\mu_0} \left(1 + \frac{2\beta}{1+\beta} \right) \right] dV$$

$$\approx \mu_0 R_\infty \left(\frac{\pi^2}{2} \frac{\tilde{P}_{-1/2}^{-1}(u_0)}{\tilde{Q}_{-1/2}^{-1}(u_0)} + \frac{3}{4} + \frac{\beta}{1+\beta} \right). \tag{13}$$

When $a/R_0 \ll 1$ and $\beta = 0$, relation (13) coincides with that used in [1,8]. In performing integral estimation (13) for the confining field, the filament as a whole does not get displaced along the major radius (global equilibrium), while the local equilibrium imposes an onerous restriction upon the local confining field (equation (3.47) from [3]).

To use the obtained solution as a CME model, in the magnetic configuration that have given rise to its AR there should be found a line almost semicircle in shape on which magnetic field $B^{(str)}$ transverse to the circle plane is approximately constant [10]. Equation (13) defines the current inside the plasma filament in the obtained field, which, in its turn, defines the filament magnetic field. The three-dimensional configuration of the total magnetic field of AR and plasma filament is shown in Fig. 2, *a* as applied to CME 2013-04-11; the plasma filament major and minor radii normalized to the solar radius were chosen equal to $R_0 = 0.2$, $a = 0.04$, the found confining magnetic field was $B^{(str)} \approx 2.7 \cdot 10^{-4}$ T. When plasma parameter $\beta = 2\mu_0 P/B_\varphi^2$ is constant, the obtained distribution of the toroidal magnetic field allows determining the pressure and, at a specified temperature T, the distribution of density $\rho \propto P/T$. Fig. 2, *b* presents the meridional cross-section of the plasma filament. In white, magnetic lines of the poloidal field (B_z, B_r) are shown (in other words, cross-sections of magnetic surfaces [3,7]). The color indicates the level of the value of rB_φ, i. e. of poloidal current whose equilibrium amplitude is to be constant over the magnetic surface [3,7]. One can see that the current isolines deviate a little from the magnetic surfaces; thus, the equilibrium is not absolute.

To achieve the equilibrium, let us substitute distributions of the fields and parameters of plasma as initial conditions

into the RMHD equations differing from the magnetic hydrodynamics equations (see [7]) in the presence of an additional retarding force with density $-\frac{\rho}{\tau}\mathbf{U}$ directed opposite to the velocity vector $\mathbf{U}$ and inducing relaxation of velocity emerging in the initially-nonequilibrium distribution during about $\tau \sim 10^3$ s. Let us consider as an example the relaxation in a uniform external field; this allows solving 2D axisymmetric RMHD equations. The result of a 6000 s evolution is presented in Fig. 2, *c* which evidently demonstrates the alignment of the current levels on magnetic surfaces and achieving a precise equilibrium. The video file (see the supplementary materials) demonstrates that the transition to equilibrium proceeds via attenuating internal oscillations. In the 3D RMHD model, the filament may also approach the 3D equilibrium via bending oscillations, and, therefore, the equilibrium shape of the filament in a real nonuniform field differs from the toroidal one.

Acknowledgements

The authors are grateful to V.S. Titov (PSI Inc., San Diego, USA) for useful discussions and acknowledge a support from the NASA LWS Strategic Capability grant 80NSSC22K0892 and NSF ANSWERS grant GEO-2149771.

Conflict of interests

The authors declare that they they have no conflict of interests.

References

[1] V.S. Titov, P. Demoulin, Astron. Astrophys., **351**, 707 (1999).
[2] J. Linker, T. Torok, C. Downs, R. Lionello, V. Titov, R.M. Caplan, Z. Mikic, P. Riley, AIP Conf. Proc., **1720**, 020002 (2016). DOI: 10.1063/1.4943803
[3] L.E. Zakharov, V.D. Shafranov, Rev. Plasma Phys., **11**, 153 (1986).
[4] P.M. Morse, H. Feshbach, *Methods of theoretical physics* (McGraw–Hill, N.Y., 1953).
[5] G.Ch. Shushkevich, Tech. Phys., **42** (4), 436 (1997). DOI: 10.1134/1.1258698.
[6] I.S. Gradshteyn, I.M. Ryzhik, *Table of integrals, series, and products* (Academic Press, N.Y., 2014).
[7] L.D. Landau, E.M. Lifshits, *Elektrodinamika sploshnykh sred* (Nauka, M., 1982). (in Russian)
[8] B. Kliem, T. Torok, Phys. Rev. Lett., **96**, 255002 (2006). DOI: 10.1103/PhysRevLett.96.255002
[9] L. Faddeev, L. Freyhult, A.J. Niemi, P. Rajan, J. Phys. A, **35**, L133 (2002). DOI: 10.1088/0305-4470/35/11/101
[10] V.S. Titov, T. Török, Z. Mikic, J.A. Linker, Astrophys. J., **790**, 163 (2014). DOI: 10.1088/0004-637X/790/2/163

Translated by Solonitsyna Anna